

Electronic Supplementary Information (ESI)

for

A chiral lanthanide metal-organic framework for selective sensing of Fe(III) ion

Xiao-Lin Zhao, Dan Tian, Qiang Gao, Hong-Wei Sun, Jian Xu* and Xian-He Bu

*School of Materials Science and Engineering, School of Chemistry, TKL of Metal- and Molecule-based
Material Chemistry, Collaborative Innovation Center of Chemical Science and Engineering (Tianjin),
Nankai University, Tianjin 300071, P. R. China*

Corresponding author Email: jxu@nankai.edu.cn

Table S1 Some selected Bond Lengths (Å) and Angles (°).

Tb-O1	2.4443	Tb-O2	2.4514
Tb-O3	2.2963	Tb-O4	2.3556
Tb-O5	2.4141	Tb-O6	2.5334
Tb-O7	2.3049	Tb-O8	2.3717
O1-Tb-O2	52.529	O1-Tb-O3	132.454
O1-Tb-O4	77.330	O1-Tb-O5	97.760
O1-Tb-O6	77.462	O1-Tb-O7	148.728
O1-Tb-O8	78.816	O2-Tb-O3	82.039
O2-Tb-O4	77.545	O2-Tb-O5	71.349
O2-Tb-O6	96.189	O2-Tb-O7	151.771
O2-Tb-O8	128.719	O3-Tb-O4	80.087
O3-Tb-O5	77.090	O3-Tb-O6	126.400
O3-Tb-O7	78.574	O3-Tb-O8	134.790
O4-Tb-O5	143.450	O4-Tb-O6	152.149
O4-Tb-O7	118.496	O4-Tb-O8	76.821
O5-Tb-O6	52.548	O5-Tb-O7	84.385
O5-Tb-O8	138.472	O6-Tb-O7	79.400
O6-Tb-O8	86.851	O7-Tb-O8	79.185

Table 2 The amounts of Tb³⁺ and Fe³⁺ ions in filter cake after washing treatment.

	Tb	Fe
In filter cake	28.9 (%)	0.18 (%)

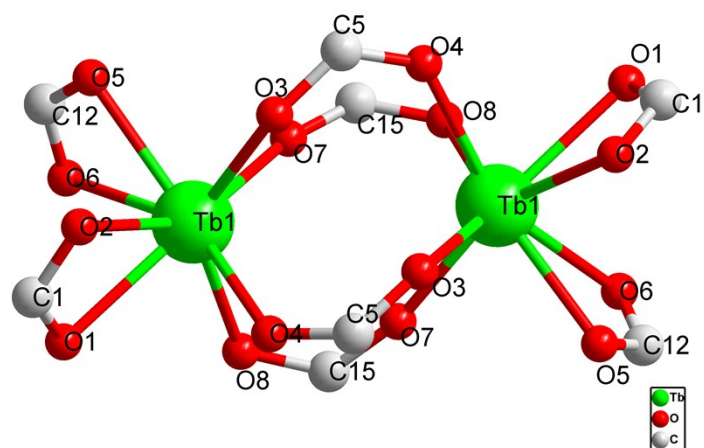


Fig. S1 The coordination environment of binuclear Tb₂ SBU.

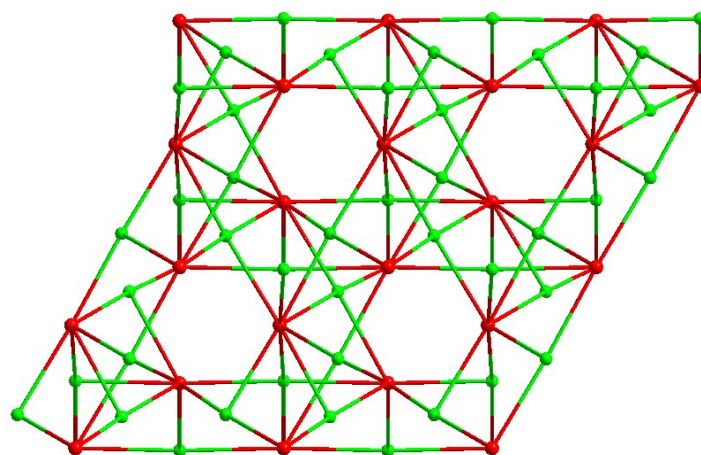


Fig. S2 The 4,8-connected net topology of compound **1** when viewing along the *c* axis.

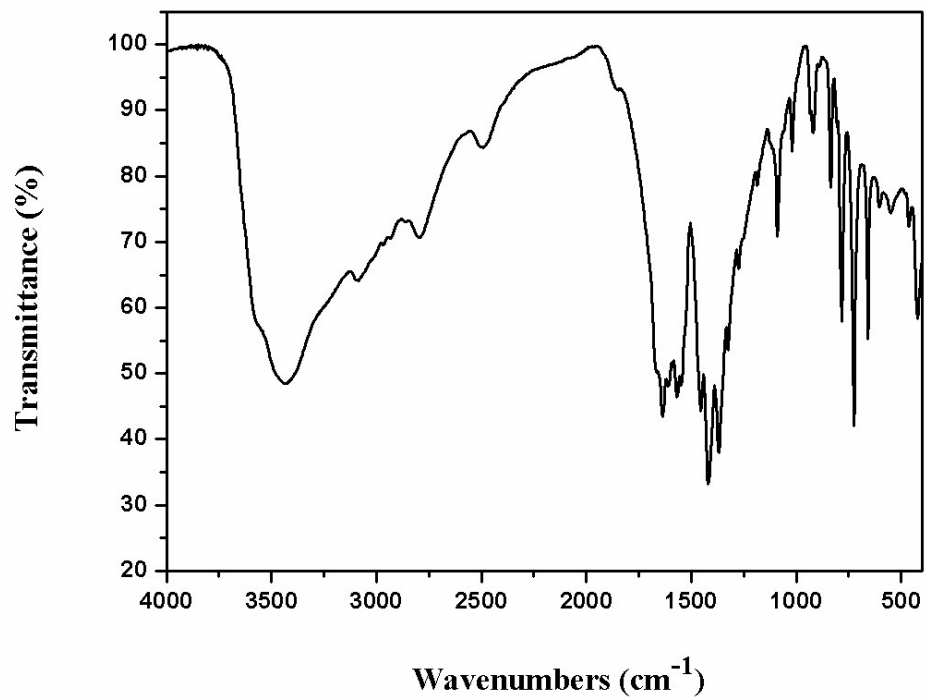


Fig. S3 The IR data for compound **1**.

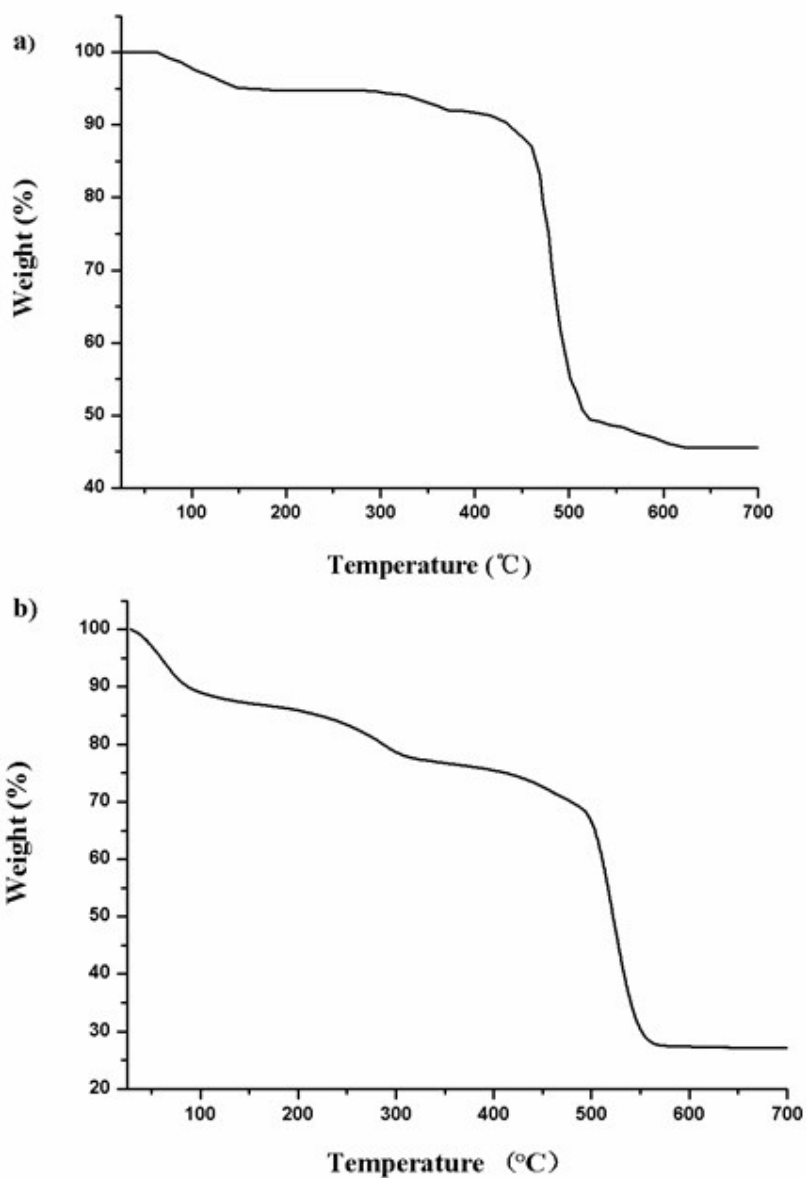


Fig. S4 The TGA curves of compound **1**. a) The TGA curve of the crystal sample exchanged with ethanol. b) The TGA curve of the crystal sample exchanged with ethanol and subsequently degassed at 160 °C in vacuum. When temperature rises up to 100 °C, the weight loss is about 10%, which coincides well with the theoretical value of the loss of H₂O molecules (Measured: 11 %, Calculated: 10.4 %).

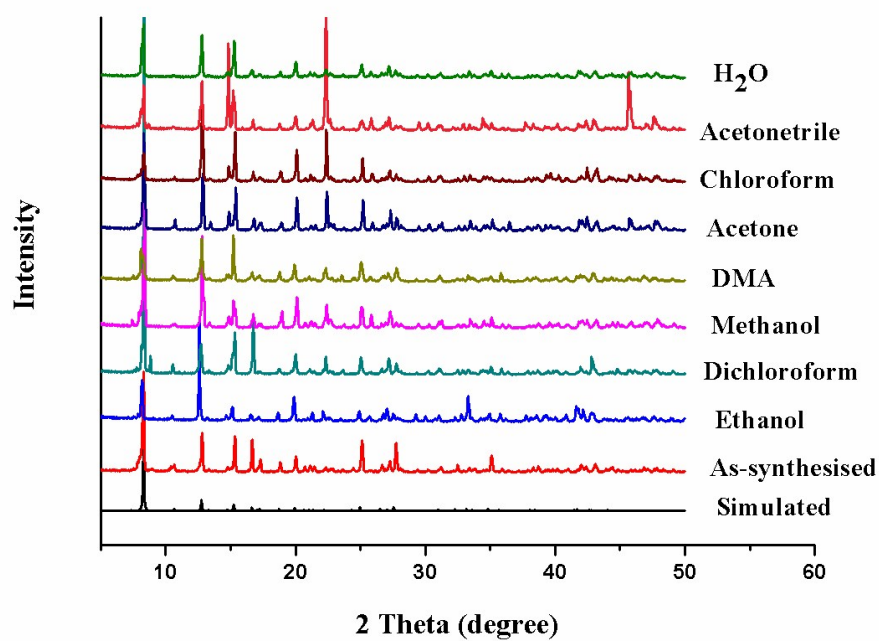


Fig. S5 The PXRD patterns of **1** after immersing in several solvents.

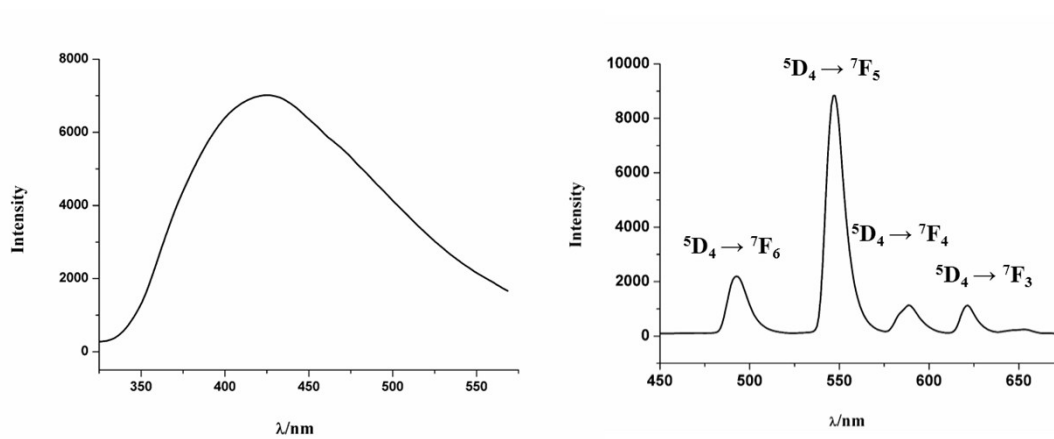


Fig. S6 The solid-state luminescence of H₄bptc ligand (left) and **1** (right).

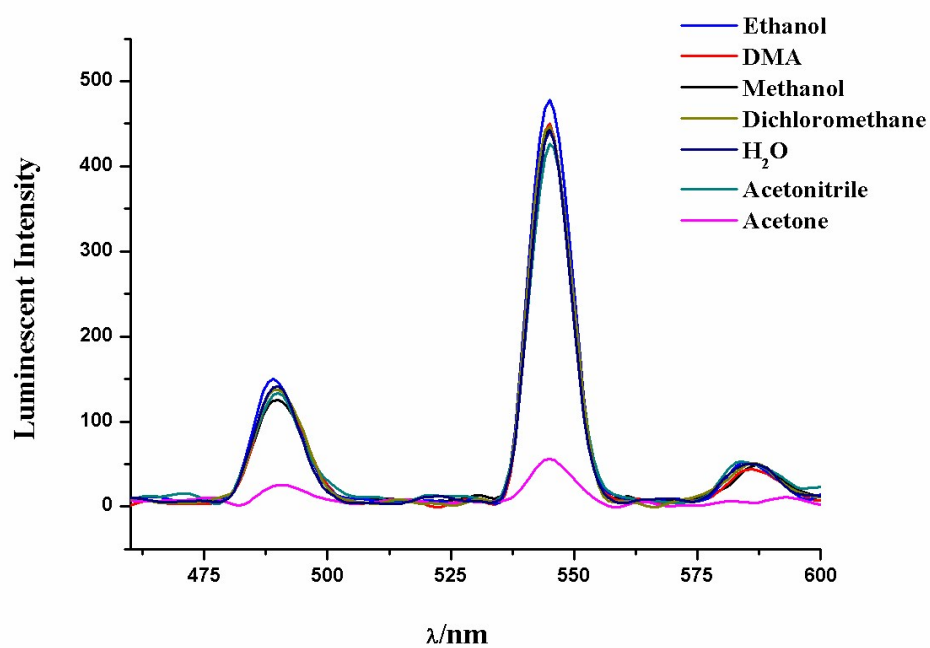


Fig. S7 The luminescence intensities of compound **1** in different solvents ($\lambda_{\text{ex}} = 310$ nm).

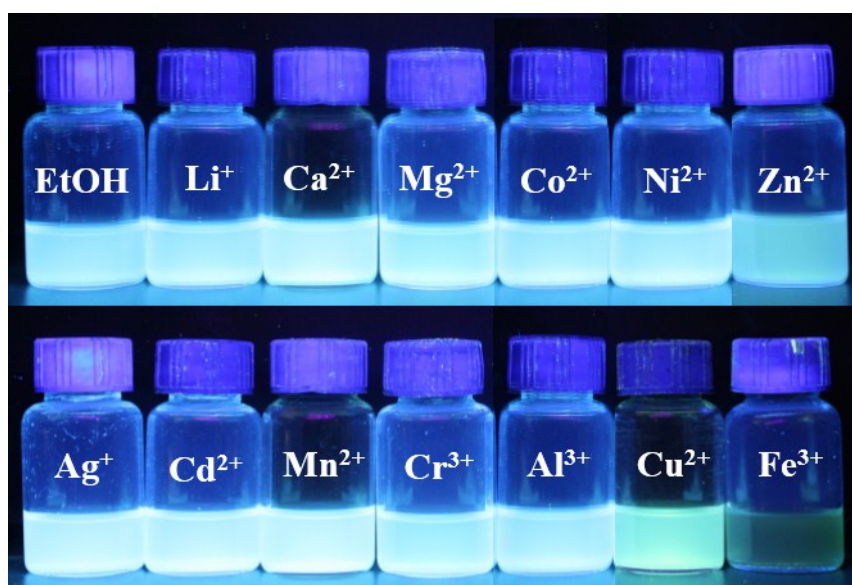


Fig. S8 The photoluminescence of **1** suspensions containing different metal ions under UV light ($\lambda_{\text{ex}} = 365$ nm).

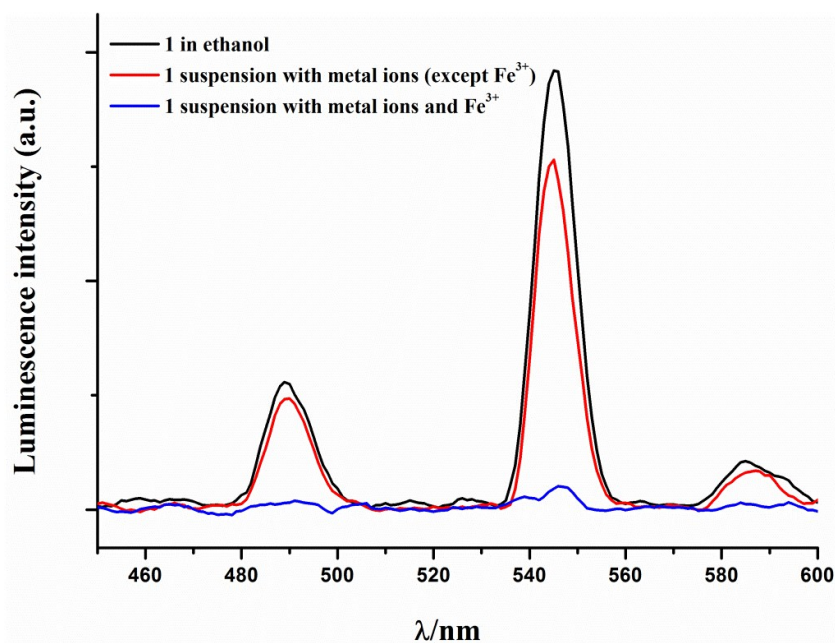


Fig. S9 The emission spectra of **1** dispersed in ethanol (black); in ethanol solution with mixed metal ions including Li^+ , Mg^{2+} , Ca^{2+} , Co^{2+} , Ni^{2+} , Zn^{2+} , Ag^+ , Cd^{2+} , Cr^{3+} , Mn^{2+} , Al^{3+} , Cu^{2+} (red); in ethanol solution with mixed metal ions and Fe^{3+} (blue).

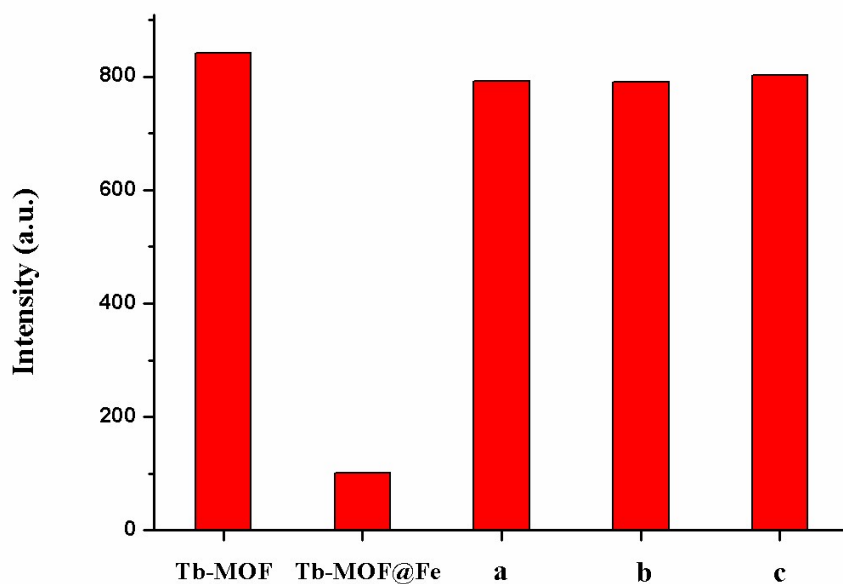


Fig. S10 The reversibility test for sensing Fe^{3+} . The luminescence intensity of Tb-MOF a) after one circle; b) after two circles; c) after three circles.

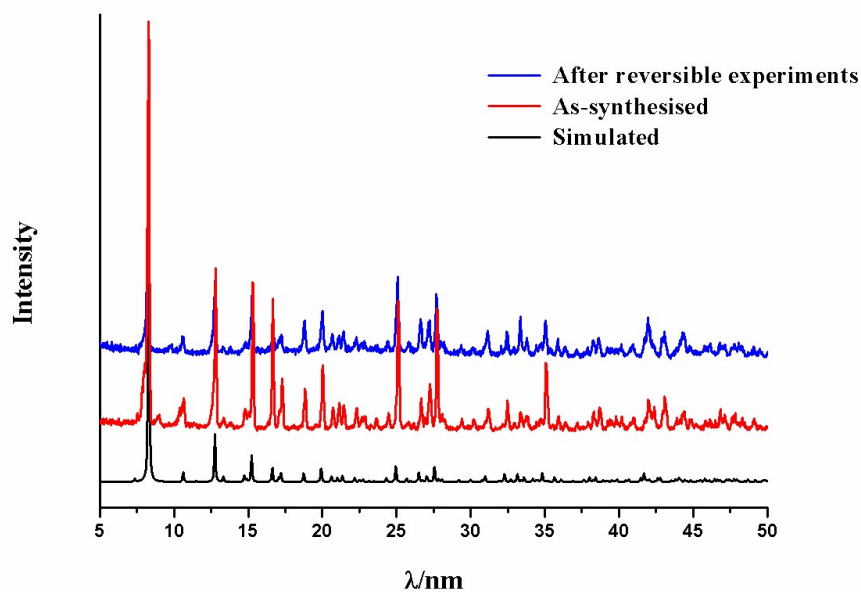


Fig. S11 The PXRD pattern of **1** after three sensing-recovery circles.

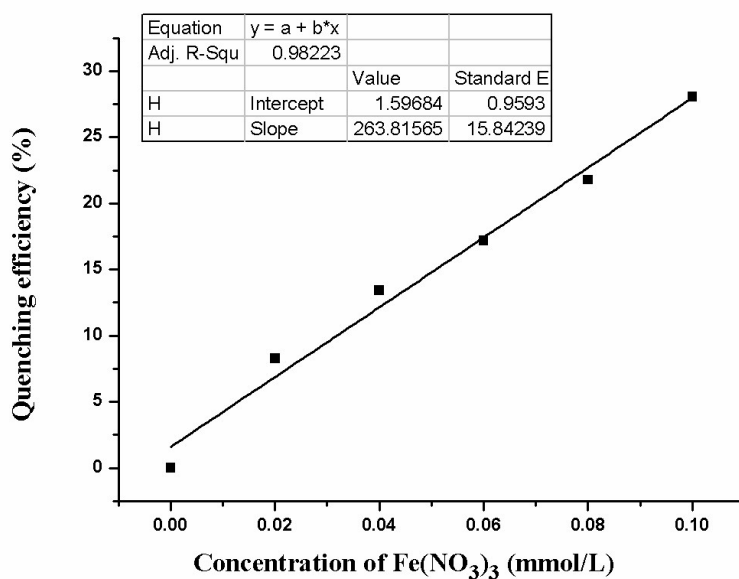


Fig. S12 The fitting plot of the quenching efficiency with the increasing concentration of Fe^{3+} in the low concentration range.

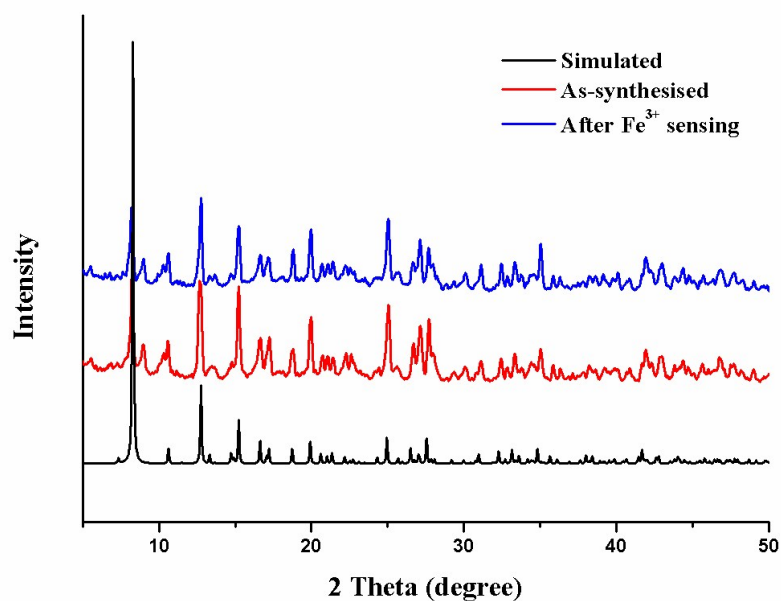


Fig. S13 The PXRD data of the as-synthesized **1** and **1** after Fe³⁺ sensing process, with the simulated result as reference.

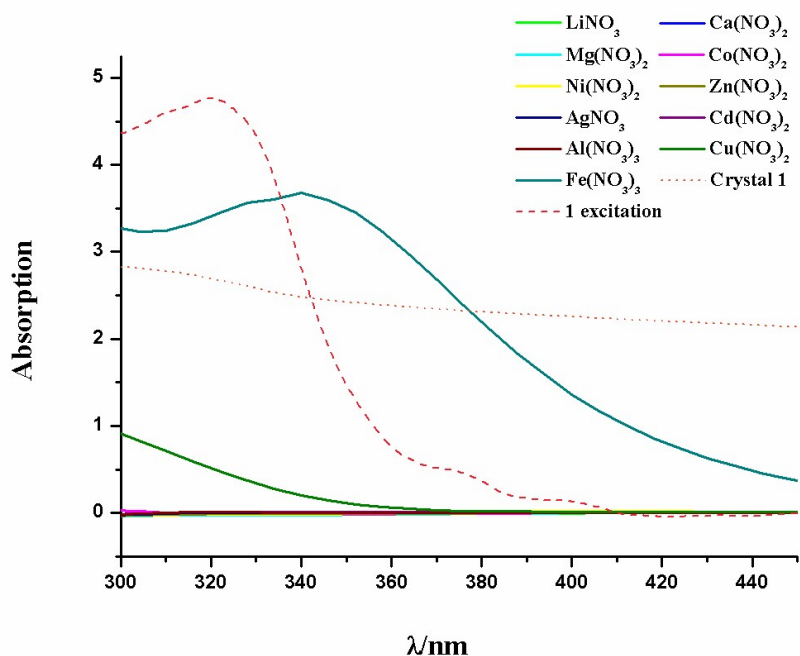


Fig. S14 Solid line: UV-vis spectra of ethanol suspensions containing different metal ions (10⁻³ mol/L); Dotted line: UV-Vis spectrum of **1** (3 mg) dispersed in ethanol (4 mL); Dashed line: Excitation spectrum of **1** (3 mg) dispersed in ethanol (4 mL).

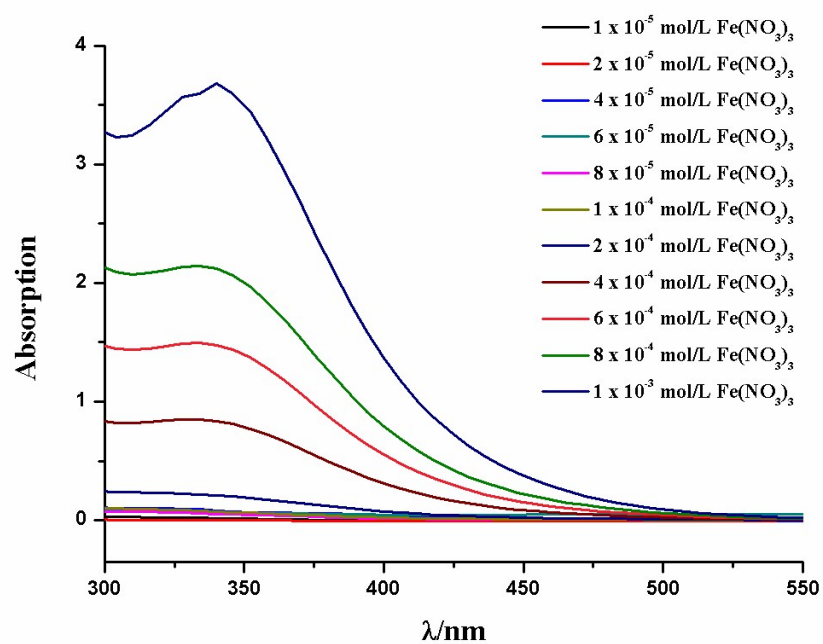


Fig. S15 The UV-vis spectra of ethanol suspensions with different concentration of $\text{Fe}(\text{NO}_3)_3$.

Note that all above luminescence experiments were carried out using the crystal sample of **1** containing enantiomers **1-D** and **1-L** simultaneously.